Design energy input spectra for high seismicity regions based on Turkish registers

F. López-Almansa · A. U. Yazgan · A. Benavent-Climent

Abstract This work proposes design energy spectra in terms of an equivalent velocity, intended for regions with design peak acceleration 0.3 g or higher. These spectra were derived through linear and nonlinear dynamic analyses on a number of selected Turkish strong ground motion records. In the long and mid period ranges the analyses are linear, given the relative insensitivity of the spectra to structural parameters other than the fundamental period; conversely, in the short period range, the spectra are more sensitive to the structural parameters and, hence, nonlinear analyses are required. The selected records are classified in eight groups with respect to soil type (stiff or soft soil), the severity of the earthquake in terms of surface magnitude M_S ($M_S \leq 5.5$ and $M_S > 5.5$) and the relevance of the near-source effects (impulsive or vibratory). For each of these groups, median and characteristic spectra are proposed; such levels would respectively correspond to 50 and 95 % percentiles. These spectra have an initial linear growing branch in the short period range, a horizontal branch in the mid period range and a descending branch in the long period range. Empirical criteria for estimating the hysteretic energy from the input energy are suggested. The proposed design spectra are compared with those obtained from other studies.

Keywords Energy spectra · Input energy · Hysteretic energy · Ductility · Nonlinear time history analysis · Turkey

F. López-Almansa (✉)
Architecture Structures Department, Technical University of Catalonia,
Avda. Diagonal 649, 08028 Barcelona, Spain
e-mail: francesc.lopez-almansa@upc.edu

A. U. Yazgan
Technical University of Catalonia, Barcelona, Spain

A. Benavent-Climent
University of Granada, Granada, Spain

1 Introduction

In the conventional earthquake-resistant design of buildings (and other constructions) the dynamic effect of the input is represented by static equivalent forces, which are obtained from acceleration response spectra defined as the ratio between the peak ground acceleration (PGA) and the maximum absolute acceleration in an equivalent Single-Degree-of-Freedom (SDOF) system. This approach entails several drawbacks: (i) these equivalent forces are strongly coupled to the elastic and hysteretic characteristics of the structure, thus making seismic design cumbersome, (ii) after the onset of yielding, correlation between the design forces and the structural damage is not feasible, and (iii) the damage caused by the cumulative inelastic excursions (Fajfar and Vidic 1994) is not accounted for. More recently, displacement-based design procedures have been proposed (Priestley et al. 2007); in these strategies, the dynamic effect of the input is represented by imposed displacements, in turn obtained from displacement response spectra relating the PGA to the maximum relative displacement in the top of the building. This formulation partially uncouples the input effect -in terms of displacement? from the characteristics of the structure and allows for a satisfactory correlation between the imposed displacement and the component of the structural damage that is related to the maximum displacement. Conversely, the component of damage that is related to the cumulative plastic strain energy cannot be appropriately considered. A more rational seismic design approach, which also overcomes this difficulty, is to express the dynamic input effect through energy response spectra. Interpreting the effect of earthquakes in terms of energy is gaining extensive attention (Housner 1956; Berg and Thomaides 1960; Kato and Akiyama 1975; Housner and Jennings 1977; Hall et al. 1984; Zahrah and Hall 1984; Akiyama 1985; Uang and Bertero 1988, 1990; Kuwamura et al. 1994; Bruneau and Wang 1996; Bertero et al. 1996; Yei and Otani 1999; Chou and Uang 2000, 2003; Adang 2007; Leelataviwat et al. 2009; Jiao et al. 2011). This approach features three major advantages: (i) the input effect in terms of energy and the structural resistance in terms of energy dissipation capacity are basically uncoupled, (ii) except in the short period range, the input energy, E_I, introduced by a given ground motion in a structure is a stable quantity, governed primarily by the natural period T and the mass m, and scarcely by other structural properties such as resistance, damping and hysteretic behavior, and (iii) the consideration of the cumulative damage fits well with this formulation and can be directly addressed. In the energy-based methods the design criterion resides in the comparison between the energy absorption capacity of the structure (i.e. its seismic resistance) and the input energy (i.e. the effect of the ground motion). It is then necessary to establish the input energy spectrum corresponding to the expected earthquake, i.e. design input energy spectrum.

This work presents energy spectra for earthquake-resistant design based on accelerograms registered in high seismicity regions of Turkey. The spectra were derived through linear and nonlinear dynamic analyses of selected Turkish accelerograms. In the long and mid period ranges the analyses are linear, given the rather low sensitivity of the spectra to structural parameters other than mass and fundamental period. Conversely, in the short period range, the spectra are more sensitive to the structural parameters, for which reason the analyses must be nonlinear, and they take constant-ductility into account.

The registers studied were selected from among those available in Turkey. The chosen records were treated (base-line correction and filtering) and classified according to the design input acceleration (e.g. the seismic zone), the soil type of the seismic station (following Eurocode 8 classification), the magnitude of the earthquake and the relevance of near-source effects, namely the velocity pulses. The design energy spectra are envelopes of the actual spectra, in terms of equivalent velocity, corresponding to each input (pair of horizontal com-

ponents); the influence of the vertical components was disregarded. These derived spectra have an initial growing branch (starting from zero) in the short period range, a horizontal branch in the mid period range and a descending branch in the long period range. Median and characteristic spectra are proposed; regardless of the statistical distribution of the spectral ordinates, such levels are intended to correspond to 50 and to 95 % percentiles, respectively.

Empirical criteria for estimating the energy input contributable to damage (hysteretic energy) from the total input energy are also suggested. These criteria mainly take into account the damping level, the degree of plastification, and the period.

The proposed design energy input spectra are compared with those obtained from other studies.

2 Seismic design based on input energy spectra

The equation of motion of a SDOF system subjected to a horizontal ground motion is given by:

$$m\ddot{y} + c\dot{y} + Q(y) = -m\ddot{z}_g \tag{1}$$

In Eq. (1) m is the mass, c is the viscous damping coefficient, $Q(y)$ is the restoring force, y is the relative displacement, and $\ddot{z}_g$is the ground acceleration. Multiplying Eq. (1) by $dy = \dot{y}\,dt$and integrating over the duration of the earthquake gives the energy balance equation

$$E_k + E_\zeta + E_a = E_I \tag{2}$$

In Eq. (2), E_k is the relative kinetic energy, E_ζ is the energy dissipated by the inherent damping, E_a is the energy absorbed by the spring, and E_I is the relative input energy:

$$E_k = \int \dot{y}\, m\ddot{y}\, dt = 1/2m\dot{y}^2 \quad E_\zeta = \int c\,\dot{y}^2 dt \quad E_a = \int Q(y)\dot{y}dt \quad E_I = -\int m\ddot{z}_g\dot{y}dt \tag{3}$$

E_a comprises the recoverable elastic strain energy, E_s, and the irrecoverable hysteretic energy E_H that represents the cumulative damage to the structure: $E_a = E_s + E_H$. In turn, the sum of E_k and $E_s$constitutes the elastic vibrational energy of the system, ($E_e = E_k + E_s$), so that Eq. (2) can be rewritten as:

$$E_e + E_\zeta + E_H = E_I \tag{4}$$

The difference between E_I and E_ζ, was denominated by Housner (1956) as the energy input that contributes to damageE_D, that is:

$$E_D = E_I - E_\zeta = E_e + E_H \tag{5}$$

At the end of the ground motion duration E_e is almost zero; consequently, from Eqs. (4) and (5) it follows that E_H can be taken as equal to E_D, i.e. $E_H \approx E_D$. Further, E_I and E_D can be normalized by the mass m and expressed in terms of equivalent velocities V_E and V_D defined by:

$$V_E = \sqrt{2E_I/m} \quad V_D = \sqrt{2E_D/m} \tag{6}$$

For a given ground motion, the relationship between the input energy E_I expressed in terms of the equivalent pseudo-velocity V_E by Eq. (5) and the natural period of the system, T, is defined as the energy input spectrum. Akiyama (1985) proposed a three-step method to obtain the design energy input spectrum for a given region from the individual energy input spectra obtained for each available ground motion record:

1. Calculate the energy input spectrum, V_E vs. T corresponding to an elastic SDOF system with 10% damping ($\zeta = 0.10$) for each ground motion recorded in the region, by quadratic combination of the energy input, in terms of equivalent velocity, obtained for the north-south, $V_{E,NS}$, and east-west, $V_{E,EW}$, horizontal components through linear dynamic response analyses, according to Eq. (3):

$$V_E = \sqrt{V_{E,NS}^2 + V_{E,EW}^2} \tag{7}$$

2. Draw a two piecewise bilinear envelope of the V_E vs. T curves. The first line goes through the origin and envelops the energy input spectra in the short period. The second line is horizontal and represents the energy input in the medium/high period range.
3. Multiply the slope of the first line by 1.20 to take into account the fact that in the short period range, the lengthening of the vibration period associated with plastification of the structure tends to increase the input energy.

It is worth emphasizing that the energy input spectrum obtained elastically is also valid for inelastic systems because the total energy input is scarcely affected by the strength and plastification level of the system, as pointed out in the Introduction. This work considers a similar approach for proposing design input energy spectra. It consists of performing the linear analyses of the first step of Akiyama's approach while the second and third steps are modified. The second step features two major modifications: (i) two envelopes are proposed, corresponding to median and characteristic values, and (ii) the envelopes are not bilinear but also contain a descending branch in the long period range. In the third step, the shifting of the slope of the initial branch is not carried out by multiplying by a constant factor; rather, the factor is derived from constant-ductility nonlinear analyses, according to Eq. (3). The registers are classified in eight groups according to the soil type (stiff or soft soil), the severity of the earthquake in terms of surface magnitude M_s ($M_s \leq 5.5$ or $M_s > 5.5$) and the relevance of the velocity pulses in the input (impulsive or vibratory).

Once E_I is determined through design energy input spectra, the energy contributing to damage E_D can be estimated through the ratio E_D/E_I. For convenience, E_D/E_I can be expressed in terms of the equivalent velocities by V_D/V_E. Past studies (Akiyama 1985; Kuwamura and Galambos 1989; Kuwamura et al. 1994; Fajfar and Vidic 1994; Manfredi 1995; Lawson and Krawinkler 1995; Teran-Gilmore 1996; Decanini and Mollaioli 2001; Benavent-Climent et al. 2002, 2010) show that V_D/V_E depends mainly on damping and ductility, and put forth empirical expressions of the ratio V_D/V_E in terms of damping and ductility parameters. The present contribution proposes a new criterion to estimate V_D/V_E that accounts for the characteristics of the above eight groups considered.

3 Turkish registers

A dataset from 1976 to 2006 (Erdogan 2008; Akkar et al. 2010) constitutes is the basis of this work. It covers 4203 registers from 2818 seismic events recorded at 327 stations. Of the 4203 registers, we selected 1320 corresponding to earthquakes with moment magnitude $M_w > 4$; among them, 540 high quality waveform registers from 131 earthquakes were taken, and finally, 149 registers with PGA $\geq$ 0.01 g corresponding to 80 earthquakes were kept for this study. The highest moment magnitude is 7.6, the Kocaeli earthquake (17/08/1999). The latest earthquakes of Kütahya-Simav (19/05/2011) and Van-Muradiye-Merkez (23/10/2011) were also included; from the Kütahya-Simav 17 registers with PGA $\geq$ 0.01 g and four registers from the Van-Muradiye-Merkez with PGA $\geq$ 0.01 g were used. Altogether, 169

registers corresponding to 82 seismic events and recorded at 90 stations are considered in this study. Every register contains horizontal (NS and EW) and vertical accelerograms; vertical components are disregarded.

Table 9 (Appendix—ESM) provides the most relevant information about the selected registers. The severity of the earthquakes is characterized by local, moment and surface magnitudes, respectively denoted by M_L, M_W, and M_S. The soil is classified as: soft soil, stiff soil or rock. When the shear wave velocity averaged in the top 30 m ($v_{s,30}$) was available (in 175 stations), the classification is based on that parameter; soft soil, stiff soil, and rock sites correspond to 180 m/s $< v_{s,30} <$ 360 m/s, 360 m/s $< v_{s,30} <$ 800 m/s and $v_{s,30} >$ 800 m/s, respectively. In the EC-8 (EN-1998 2004), these three categories respectively correspond to ground types C, B and A. Because there are no stations with $v_{s,30} <$ 180 m/s, this study does not cover soil types D and E. In five stations the soil classification is not based on $v_{s,30}$ and in 13 stations the soil type was not known and the corresponding 13 registers were disregarded. In view of the Turkish design code (TSC 2007), for seismic zones 1, 2 and 3, the design seismic acceleration is 0.4, 0.3 and 0.2 g, respectively. R_{jb}, R_{rup} and R_{epi} respectively correspond to Joyner–Boore, rupture and epicentral distances (Erdogan 2008). Bracket duration (t_{br}) (Kempton and Stewart 2006) is comprised between the instants when 5 % of the maximum acceleration is exceeded for the first and last time. Triffunac duration (Triffunac and Brady 1975) (t_{tf}) corresponds to the time interval in between 5 and 95 % of integral $\int \ddot{z}_g^2 dt$. The Arias intensity I_A (Arias 1970) constitutes a measure of the destructive capacity of an accelerogram and is defined as

$$I_A = \frac{\pi}{2g} \int \ddot{z}_g^2 dt \tag{8}$$

The impulsivity of a given accelerogram can be detected in several ways (Baker 2007). The dimensionless index I_D (Manfredi 2001) is a frequently used indicator defined by

$$I_D = \frac{\int \ddot{z}_g^2 dt}{\ddot{z}_g^{max} \dot{z}_g^{max}} \tag{9}$$

The integral extends to the ground motion duration. In the references (Iervolino et al. 2006; Cosenza et al. 2009) several threshold values of I_D are suggested. In this work it is assumed that $I_D < 10$ and $I_D > 10$ correspond to impulsive and to vibratory ground motions, respectively.

The registers are treated with baseline correction and with bi-directional, zero-shift ("acausal"), 4th-order Butterworth filtering. The purpose of the band-pass filtering is to remove long-period and short-period noise. The low and high-cut frequencies are decided case-by-case using an iterative procedure, carried out on the Fourier spectra, until the resulting velocity and displacement traces are considered visually acceptable. The low-cut frequency generally ranges between 0.05 and 0.5 Hz (2 and 20 s), while the high-cut frequency ranges from 15 to 40 Hz (0.067 and 0.025 s). This information is indicated in last two columns of Table 9. Although most of the information was taken from (Erdogan 2008), the values of the bracket and Triffunac durations, and the Arias and dimensionless indexes were determined in this study (Table 9).

Figure 1 displays the location and the soil type of the 90 stations that correspond to registers in Table 9; three of them correspond to rock, 35 to stiff soil, 42 to soft soil, and in 10 the soil type is not known. This information is superposed on the design peak ground acceleration established by the Turkish seismic design code (TSC 2007).

Figure 1 shows that most of the registering stations lie inside zone 1, i.e. the highest seismicity region of Turkey.

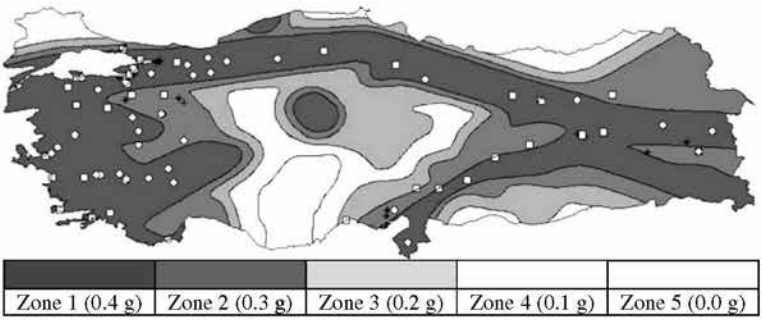

Fig. 1 Location and soil type of the registering stations. Rock: "*Plus*". Stiff soil: "*square*". Soft soil: "*circle*". Unknown: "*asterisk*"

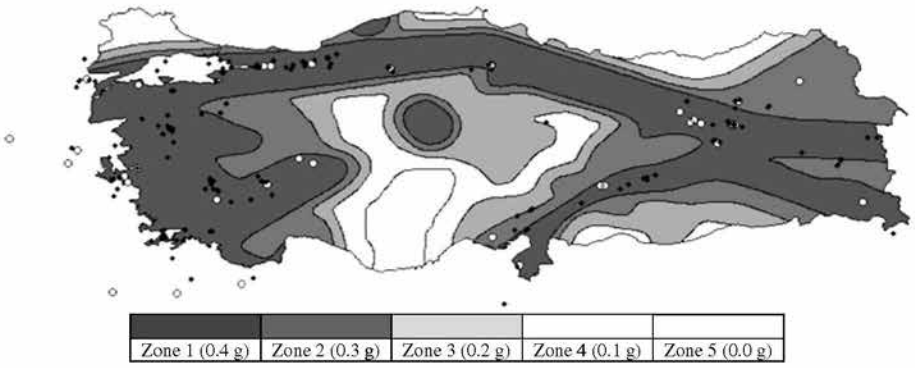

Fig. 2 Locations of the epicenters and magnitudes of the earthquakes. $M_S \leq 5.5$: "*filled diamond*". $M_S > 5.5$: "*circle*"

Figure 2 displays the location of the epicentres of the 82 earthquakes together with their magnitude.

As seen in Fig. 2, a considerable number of the epicenters are located inland, which means that important near-source effects can be expected; this is confirmed by the number of impulsive registers in Table 9.

The registers in Table 9 are classified into 12 groups in light of the following factors:

- **Soil type**. The three aforementioned soil types (rock / stiff soil / soft soil) are considered.
- **Magnitude of the earthquake**. Eurocode 8 (EN-1998 2004) proposes two different design spectra, designated as Type 1 and Type 2, corresponding to registers from earthquakes with surface magnitudes higher and smaller than 5.5, respectively. Accordingly, the registers in Table 9 are classified as produced by earthquakes with $M_S > 5.5$ or $M_S \leq 5.5$.
- **Near-fault effects**. Impulsive and vibratory registers are considered separately; as mentioned after Eq. (9), these categories correspond to $I_D \leq 10$ and to $I_D > 10$, respectively.

Given the scarcity of results corresponding to rock, it was decided to focus this study on stiff soil and soft soil. Therefore, eight groups of registers were finally analyzed: stiff soil / soft soil, $M_S > 5.5$ / $M_S \leq 5.5$ and impulsive / vibratory. For rock, some incomplete results about design spectra are also proposed, however, and the lack of seismic information for Turkey is partially compensated by other sources.

4 Proposal of design input energy spectra

4.1 Introductory remarks

This section describes the proposal of design input energy spectra in terms of velocity, V_E. These spectra are intended for structures with both linear and nonlinear behavior, respectively addressed in Subsects. 4.2 and 4.3. The linear spectra are derived from linear dynamic analyses of the registers listed in Table 9. As indicated in the Introduction, in the mid and long period ranges the input energy is a rather stable quantity, primarily governed by the total mass and fundamental period T of the structure, and scarcely affected by its strength or hysteretic properties; therefore, in these period ranges the linear spectra can also be used for nonlinear design. Conversely, the energy spectral ordinates in the short period range are not as clearly independent of the resistance and hysteretic behavior, making necessary nonlinear dynamic analyses. The nonlinear spectra are proposed to be roughly equal to the linear ones in the mid and long period ranges, whereas in the short period range their ordinates are obtained by modifying those of the linear spectra with factors adequate to this end.

The linear and nonlinear spectra are proposed for each of the aforementioned eight groups (stiff soil / soft soil, impulsive / vibratory, $M_s > 5.5/M_s \leq 5.5$); given the scarcity of registers out of the seismic zone 1 (see Fig. 1) and their rather low intensity (see Table 9), only inputs from zone 1 are considered. For each group, median and characteristic spectra were established as the 50 and 95 % percentiles, respectively. As the obtained spectra (Yazgan 2012) are not seen to fit any statistical distribution, the median and characteristic values were determined regardless of their distribution.

4.2 Linear spectra

Given the similarity between the relative velocity spectra and V_D spectra (Housner 1956; Akiyama 1985) and the limited sensitivity of ratio V_D/V_E to the period (Decanini and Mollaioli 2001; Benavent-Climent et al. 2010), the proposed spectra are expected to be basically shaped as the result of multiplying the design acceleration spectra according Eurocode 8 (EN-1998 2004) by the factor $T/2\pi$. Therefore, these spectra have three branches, corresponding roughly to the short, medium and long period ranges. The first branch is linear and starts from zero, the second branch is constant, and the third branch decreases. Figure 3 offers a sketch, where T_C and T_D are the corner periods separating the three branches.

In Fig. 3 the descending branch (for $T \geq T_D$) follows the equation

$$V_E = V_E^{max} \left(\frac{T_D}{T} \right)^a \tag{10}$$

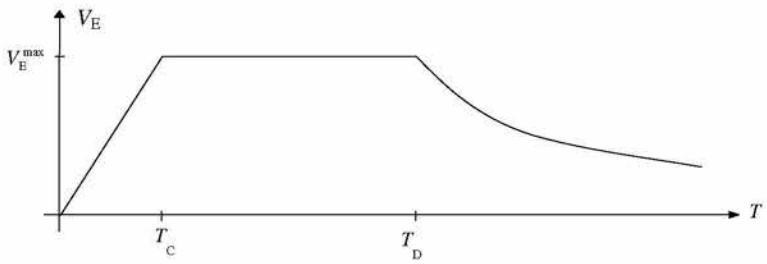

Fig. 3 Proposed linear V_E design spectra

In Eq. (10), V_E^{max} is the spectral ordinate of the plateau and a is an exponent. Figure 3 and Eq. (10) show that every proposed linear spectrum is characterized by the periods T_C and T_D, by the plateau ordinate V_E^{max} and by the exponent a.

The proposal of the linear design input energy spectra in terms of velocity (V_E) in the range of periods 0–T consists of deriving separately normalized spectra ($V_E \parallel V_E \parallel_T$) and norms ($\parallel V_E \parallel_T$); the proposed V_E design spectra are obtained by multiplying the normalized spectra by the norms. This makes it possible to perform statistical studies on individual spectra obtained from registers of different intensities. The norm $\parallel V_E \parallel_T$ is defined as the integral of the V_E spectrum:

$$\| V_E \|_T = \int_0^T V_E dT \tag{11}$$

The normalized spectra are obtained from the linear analyses carried out on the Turkish registers listed in Table 9. However, given the scarcity of available strong inputs, the norms are obtained from the Turkish recordings only in the group where the inputs are more demanding ("Soft Soil / $M_s > 5.5$ / Impulsive"). For the other groups, the available registers are too small, and this lack of seismic information is offset with information from previous studies (Decanini and Mollaioli 1998) and major design codes (EN-1998 2004; BSL 2009; UBC 1997). The linear analyses consisted of determining the value of E_I in Eq. (3) for SDOF systems with damping factor $\zeta = 0.10$ and for natural T periods between 0.02 and 8 s.

Below we specify the criteria for estimating, for each of the eight groups (Sect. 3), the values of parameters T_C, T_D, $V_E^{max} / \| V_E \|_T$ and a that characterize every normalized spectrum. The spectra with the smallest norms, corresponded to minor registers, were disregarded.

- **Period T_C**. For each of the eight groups, the procedure to estimate the median and characteristic values of the corner period T_C involved the following consecutive steps: (i) for each individual normalized spectrum, T_C is initially defined as the intersection between the initial envelope (linear envelope starting from the origin) and the horizontal (maximum) envelope; (ii) for all the individual normalized spectra considered in this group, the median and characteristic values of such T_C periods are determined. The initial median and characteristic branches are finally obtained by joining the origin and the points of the above maximum linear envelopes corresponding to the median and characteristic values of T_C, respectively.
- **Period T_D**. Eurocode 8 proposes separate design spectra for registers corresponding to $M_s > 5.5$ (Type 1) and to $M_s \leq 5.5$ (Type 2), though T_D does not depend on the soil type in eithr case. In this study, the same value for T_D is used for all types of soil. Eurocode 8 specifies T_D = 2 s and T_D = 1.2 s for Type 1 and Type 2 spectra, respectively, whereas for our purposes values T_D = 1.6 s and T_D = 0.9 s provided better fits and were adopted for registers corresponding to $M_s > 5.5$ and to $M_s \leq 5.5$, respectively. These values are taken regardless of the soil type and the near-source effects, and no distinction is made between median and characteristic spectra.
- **Plateau ordinate $\mathbf{V_E^{max} / \| V_E \|_T}$**. For each of the eight groups, the median and characteristic maximum normalized spectral ordinates $V_E^{max} / \| V_E \|_T$ are respectively estimated as the average, in the range $T_C - -T_D$, of the median and characteristic values of the normalized spectra. The individual spectra having the smallest norms were disregarded in this operation.
- **Exponent a**. For each group, the exponent a is determined as providing the best fit, in the range $T_D - T$.

Table 1 Parameters for the median/characteristic normalized spectra $V_E \parallel V_E \parallel_4$

Soil type	Magnitude	Pulses	n	T_C (s)	T_D (s)	$V_E^{max} / \parallel V_E \parallel_4$ (s^{-1})	a
Stiff soil	$M_s > 5.5$	Impulsive	12	0.41 / 0.18	1.60 / 1.60	0.28 / 0.46	0.55 / 0.5*
		Vibratory	5	0.22 / 0.17	1.60 / 1.60	0.35 / 0.47	1.0 / 1.2
	$M_s \leq 5.5$	Impulsive	8	0.30 / 0.20	0.90 / 0.90	0.52 / 0.85	1.3 / 1.5
		Vibratory	9	0.27 / 0.19	0.90 / 0.90	0.49 / 0.78	1.2 / 1.2
Soft soil	$M_s > 5.5$	Impulsive	19	0.54 / 0.32	1.60 / 1.60	0.34 / 0.53	1.0 / 0.8*
		Vibratory	13	0.53 / 0.28	1.60 / 1.60	0.33 / 0.50	0.9 / 0.65
	$M_s \leq 5.5$	Impulsive	11	0.29 / 0.21	0.90 / 0.90	0.46 / 0.70	0.9 / 1.0
		Vibratory	18	0.26 / 0.18	0.90 / 0.90	0.41 / 0.69	0.7 / 0.9

* These values were modified to fit the peaks inside the range from 4 to 8 s

Since most civil engineering constructions correspond to periods not exceeding 4 s, in this study $T = 4$ s, that is, the proposed design spectra are limited to the range 0–4 sec. However, the linear dynamic analyses were carried out in the interval 0–8 sec. When relevant peaks were detected for periods $4 < T < 8$ seconds, this information was considered for modifying the descending branch. For each of the eight groups, Table 1 gives the actual number of registers (n) and the values of parameters T_C, T_D, $V_E^{max} / \parallel V_E \parallel_T$ and a, for the median / characteristic $V_E \parallel V_E \parallel_4$ normalized spectra. Figure 4 displays the spectra. Each of the eight groups of plots inside Fig. 4 contains the individual normalized spectra (thin gray lines), the median and characteristic ones (bold gray lines) and the proposed (smoothed) median and characteristic normalized spectra (black bold lines).

As stated previously, the proposed V_E design linear spectra are determined by multiplying the smoothed (three-branched) normalized spectra shown in Fig. 4 by norm $\parallel V_E \parallel_4$. Table 2 aims to highlight this process by displaying the values of $\parallel V_E \parallel_4$ and of the ordinate values for the constant-velocity branches of several V_E spectra, i.e. their plateau ordinates V_E^{max}; the left/right figures represent median/characteristic values, respectively. The fourth column of Table 2 shows the values of norm $\parallel V_E \parallel_4$ obtained in this study as the average of the largest registers in each group (Yazgan 2012). The fifth column contains the spectral values described in the reference (Decanini and Mollaioli 1998) and the sixth, seventh and eighth columns contain the design quantities according to the Eurocode 8 (EN-1998 2004), the Japanese code (BSL 2009) and the UBC-97 (UBC 1997). In all these codes, the design ground acceleration is 0.4 g. Further details are given below.

- Decanini and Mollaioli (1998). These researchers described design spectra in terms of input energy normalized with respect to the mass (E_I/m); the corresponding V_E value in Table 2 was determined using Eq. (6). The design spectra were based on linear analyses of numerous seismic strong motions world-wide, classified by soil conditions, earthquake magnitude and source-to-site distance. The values shown in Table 2 were selected to represent similar conditions. Decanini and Mollaioli specified S1, S2 and S3 soil types; the "rock" and "stiff soil" in this work match their S1 while "soft soil" matches S2. Since the values proposed for soil S1 stand for the most demanding situation in this category, we assigned these values to "stiff soil" rather than "rock". The values for earthquake magnitude, as shown in Table 2, were $M_s > 5.5$ for the interval 6.5–7.1 and $M_s \leq 5.5$ for the interval 4.2–5.2. The values indicated for impulsive and vibratory registers are consistent with source-to-site distances smaller than 5 km, and between 12 and 30 km, respectively. In Table 2, left figures are mean values and the right ones give the mean + standard deviation.

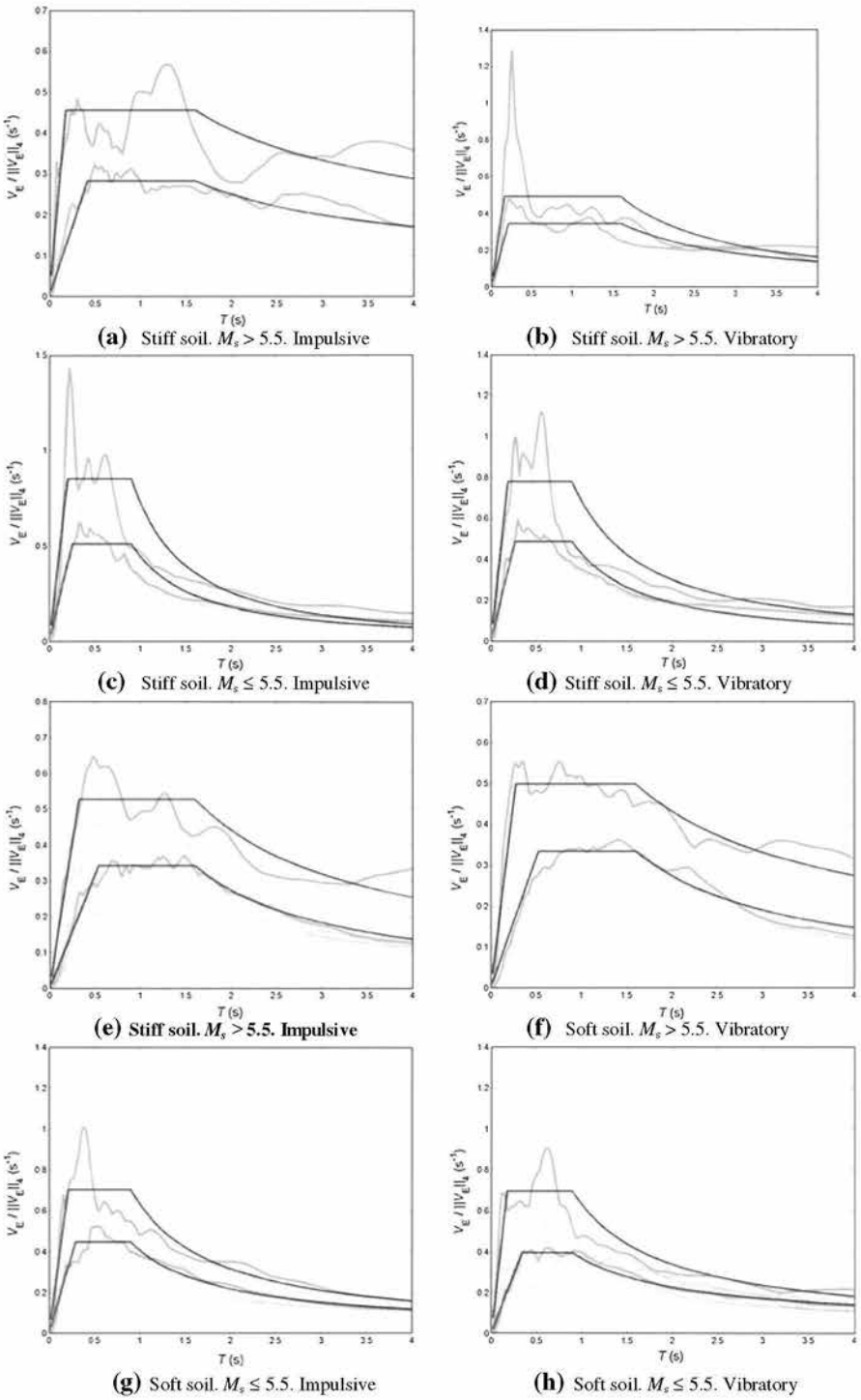

(a) Stiff soil. $M_s > 5.5$. Impulsive

(b) Stiff soil. $M_s > 5.5$. Vibratory

(c) Stiff soil. $M_s \leq 5.5$. Impulsive

(d) Stiff soil. $M_s \leq 5.5$. Vibratory

(e) **Stiff soil. $M_s > 5.5$. Impulsive**

(f) Soft soil. $M_s > 5.5$. Vibratory

(g) Soft soil. $M_s \leq 5.5$. Impulsive

(h) Soft soil. $M_s \leq 5.5$. Vibratory

Fig. 4 Proposed normalized $V_E \parallel V_E \parallel_4$ design spectra

Table 2 Mean/characteristic ordinates of the constant-velocity branches of the V_E spectra

Soil type	Magnitude	Velocity pulses	$\| V_E \|_4$ (cm)	(V_E^{max}) (cm/s)					
				Decanini and Mollaioli (1998)	Eurocode 8	Japanese code	UBC-97	This study	Proposal
Rock	$M_S > 5.5$	Impulsive	–	–	–	–	– / 142	–	168 / 260
		Vibratory	–	–	– / 89	– / 234	– / 88	–	84 / 129
	$M_S \leq 5.5$	Impulsive	–	–	–	–	– / 88	–	51 / 80
		Vibratory	–	–	– / 56	– / 234	– / 88	–	28 / 43
Stiff soil	$M_S > 5.5$	Impulsive	200	312 / 361	–	–	– / 199	56 / 93	235 / 364
		Vibratory	47	155 / 179	– / 133	–	– / 123	17 / 22	117 / 181
	$M_S \leq 5.5$	Impulsive	71	95 / 110	–	–	– / 123	37 / 60	72 / 112
		Vibratory	22	52 / 60	– / 75	–	– 123	11 / 17	39 / 60
Soft soil	$M_S > 5.5$	Impulsive	746	338 / 419	–	–	– / 227	**255 / 395**	255 / 395
		Vibratory	208	228 / 283	– / 153	– / 312	– / 142	69 / 104	172 / 266
	$M_S \leq 5.5$	Impulsive	59	129 / 160	–	–	– / 142	27 / 41	97 / 150
		Vibratory	50	72 / 89	– / 83	– / 312	– / 142	21 / 34	54 / 84

- **Eurocode 8**. Since Eurocode 8 does not directly establish energy input spectra, V_E values were estimated by identifying the V_D spectra with the pseudo-velocity design spectra (S_v); their ordinates were determined by multiplying those of the acceleration design spectra S_a by $T/2\pi$. Input energy in terms of velocity (V_E) was derived from V_D by means of the left-hand Eq. (14) (Akiyama 1985). Magnitudes higher than 5.5 correspond to Type 1 spectra and those smaller than 5.5 are consistent with Type 2 spectra. Since Eurocode 8 does not contain any specific indication about directivity effects or the probability of exceeding the spectral ordinate, the obtained quantities were assigned to vibratory registers and to characteristic values.
- BSL (2009). The Japanese code provides energy input spectra directly in terms of V_D; the V_E spectra were obtained from V_D spectra as in Eurocode 8. The soil is classified in types 1, 2 and 3. Type 1 is considered to be equivalent to "rock" and type 2 matches the conditions of both "stiff soil" and "soft soil"; since the values for type 2 should correspond to the most demanding situation inside this category, they have been assigned to "soft soil".
- UBC (1997). Like Eurocode 8, the UBC-1997 code proposes energy input spectra indirectly, through absolute acceleration S_a response spectra. The input energy in terms of equivalent velocity (V_E) was accordingly determined along the lines of Eurocode 8. Soil is classified in six types, S_A to S_F; S_B is equivalent to "rock", S_C is "stiff soil" and S_D matches the conditions of "soft soil". Registers generated by earthquakes with $M_s > 5.5$ and with $M_s \leq 5.5$ are respectively identified with types A and C. For earthquakes with $M_s > 5.5$, the values for impulsive registers can be obtained by multiplying those of the vibratory ones by a factor N_v; under UBC-1997, it is assumed that $N_v = 1.6$.

The ninth column of Table 2 contains the constant-velocity spectral ordinates V_E^{max} obtained in this study for seismic zone 1 in Turkey (design ground acceleration 0.4 g) obtained by multiplying the normalized ordinates $V_E^{max}/\|V_E\|_4$ given in the seventh column of Table 1 by norm $\| V_E \|_4$ in the fourth column of Table 2. Comparison of the obtained quantities and the figures in the previous four columns shows that only the group "Soft Soil / $M_s > 5.5$ / Impulsive" contains sufficient strong registers for highly demanding results; in the other groups, the obtained spectral ordinates are too small to represent the actual seismicity of Turkey. This lack of data calls for complementary information from the previous four columns, mainly the first one. Accordingly, the final column in Table 2 displays the constant-velocity spectral ordinates V_E^{max}proposed in this study for seismic zone 1 in Turkey. The proposed median values were determined taking into account columns five through eight, while the characteristic values were derived from the median ones by assuming that the median/characteristic ratios are the same as in the group "Soft Soil / $M_s > 5.5$ / Impulsive" that is, 255/395 = 0.646. This assumption stems from the consideration that the statistical properties are basically independent of soil type, earthquake magnitude and source-to-site distance. For stiff and soft soil, the median values were determined using the mean values of Decanini and Mollaioli and adopting the proportion of group "Soft Soil / $M_s > 5.5$ / Impulsive", which is 255/338 = 0.754. In contrast, for rock, we arrived at the median and characteristic values by dividing those proposed for stiff soil by 1.4, as indicated under UBC-97 (seventh column) for earthquakes with $M_s > 5.5$.

The proposed V_E design linear spectra are shaped like the normalized spectra shown in Fig. 4, but the plateau ordinates V_E^{max} are taken from Table 2. Figure 5 displays the proposed V_E linear spectra corresponding to stiff soil and to soft soil; the unscaled individual spectra used to derive the design ones are also plotted for comparison. In the case of rock, available

information did not allow for deriving V_E design spectra aside from the plateau ordinates indicated in Table 2.

The spectra drawn in Fig. 5 correspond to seismic zone 1 in Turkey, whose design input acceleration is 0.4 g; in the other seismic zones of Turkey (and of other countries), the design spectra can be obtained by multiplying the spectral ordinates by the ratio between the actual design acceleration and 0.4 g.

4.3 Nonlinear spectra

As discussed in Sect. 2, the proposed V_E nonlinear spectra are similar to the linear ones except in the short period range, where the energy input in a nonlinear SDOF system with initial period T is larger than that of the counterpart elastic system with the same period of vibration, due to the elongation of the fundamental period of the structure generated by the nonlinear behavior. This causes a shortening of the corner period T_C that results in an increase of the slope of the initial branch. Akiyama (1985) suggested deriving the slope of the initial branch of the nonlinear spectra by multiplying the slope of the linear spectra by 1.2, a factor derived from a limited number of records; the authors believe a more precise evaluation is required because many low-to-medium rise buildings have fundamental periods in the range 0–T_C. The nonlinear time history analyses consist of determining the value of E_I given by Eq. (3) in the range 0–4 s for the inputs listed in Table 9. The considered nonlinear SDOF systems have an elastic-perfectly plastic behavior and are therefore characterized by their damping ratio ζ, by their initial (elastic) natural period T, and by the displacement ductility μ. In this study, three values of ζ are considered (0.02, 0.05, 0.10) and six values of μ are considered (2, 3, 5, 10, 15, 20). Obtaining the spectrum of each acceleration record for a given fixed value of μ calls for performing iterative analyses in which the yield strength of the SDOF system, Q_y, is varied until the resulting μ reaches the prescribed target value with 10 % tolerance. Since the accelerograms corresponding to NS and EW directions are considered separately, the total number of spectra obtained is $338 \times 3 \times 6 = 6084$. As discussed in the next section, these spectra are also used for estimating the ratio V_D / V_E.

For each nonlinear analysis the slope of the initial smoothed branch is obtained as the best linear fit in the range 0- T_C, and this slope is termed m. Figure 6 displays, in thin dashed lines, some values of the ratio m/m_1 that correspond to $\zeta = 0.05$; m_1 is the linear slope, i.e. corresponding to $\mu = 1$. The work (Yazgan 2012) shows the omitted plots and similar results for $\zeta = 0.02$ and 0.10. Given the high scattering of the values shown in Fig. 6, these ratios cannot be used to modify the linear spectra; rather, they must be averaged and smoothed. The thick dashed lines in Fig. 6 represent the median values, i.e. corresponding to the 50 % percentile. Since these lines are too abrupt, they can be smoothed by means of the following equation (Benavent-Climent et al. 2010):

$$\frac{m_\mu}{m_1} = p(\mu - 1) + \frac{(1 + r)\,\mu^s}{r + \mu^s} \tag{12}$$

In this study, parameter r is taken to be $r = 0.3$, while parameters p and s are determined the ones providing the best fit with the median values (thick dashed lines in Fig. 6); the resulting values are indicated in Table 3. The smoothed ratios $m\mu/m_1$ are drawn with thick solid lines in Fig. 6. Table 4 displays the smoothed factors $m\mu$ / m_1 that will modify the slopes of the initial branches of the linear V_E spectra.

Table 4 shows that the m_μ/m_1 ratios are greater for higher values of μ, and that for mid and large values of μ, the ratios m_μ/m_1 tend to be higher for impulsive registers than for vibratory ones. Comparison of the constant value 1.2 suggested by Akiyama and the factors

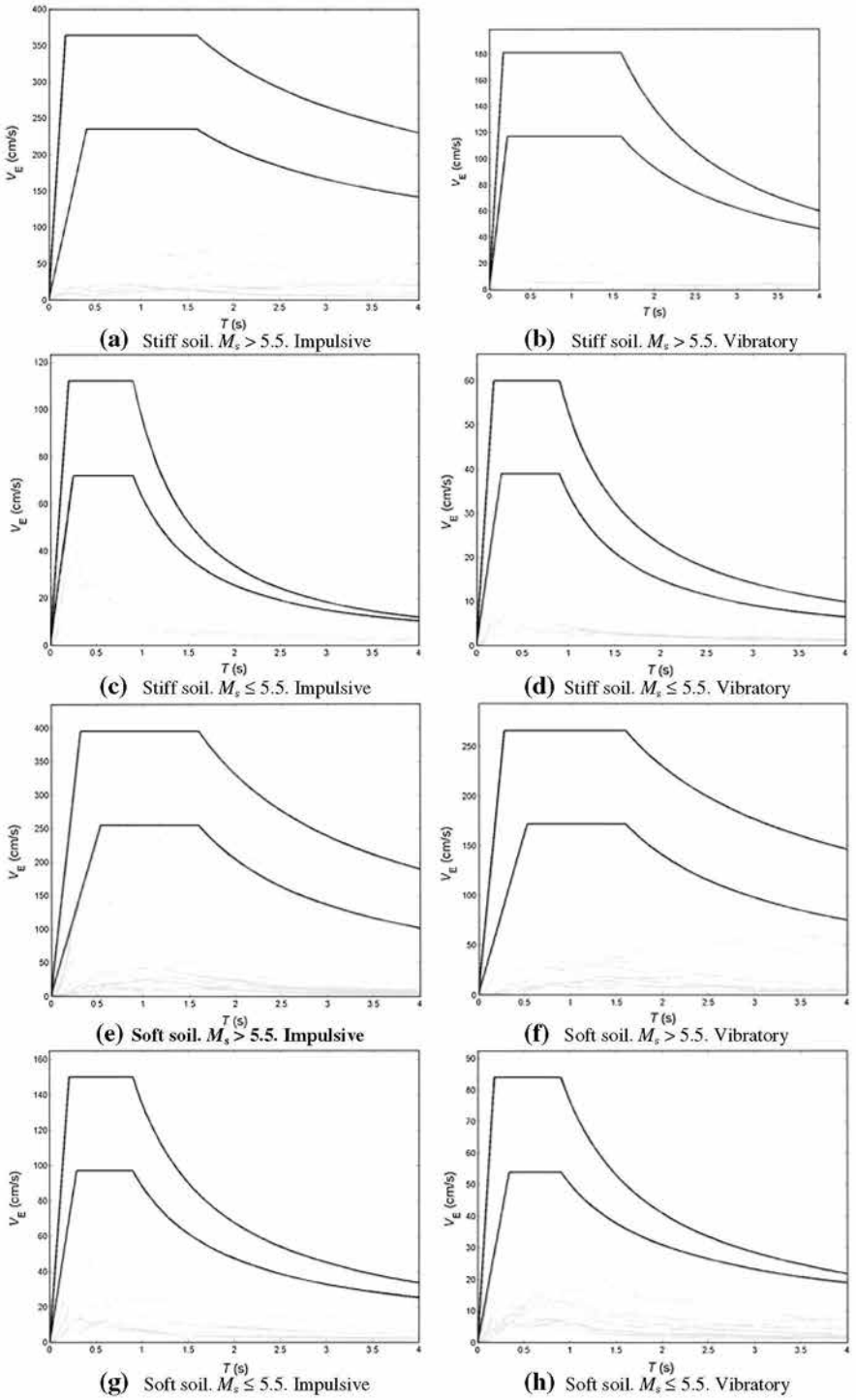

(a) Stiff soil. $M_s > 5.5$. Impulsive

(b) Stiff soil. $M_s > 5.5$. Vibratory

(c) Stiff soil. $M_s \leq 5.5$. Impulsive

(d) Stiff soil. $M_s \leq 5.5$. Vibratory

(e) **Soft soil. $M_s > 5.5$. Impulsive**

(f) Soft soil. $M_s > 5.5$. Vibratory

(g) Soft soil. $M_s \leq 5.5$. Impulsive

(h) Soft soil. $M_s \leq 5.5$. Vibratory

Fig. 5 Linear V_E design spectra proposed for design acceleration 0.4 g

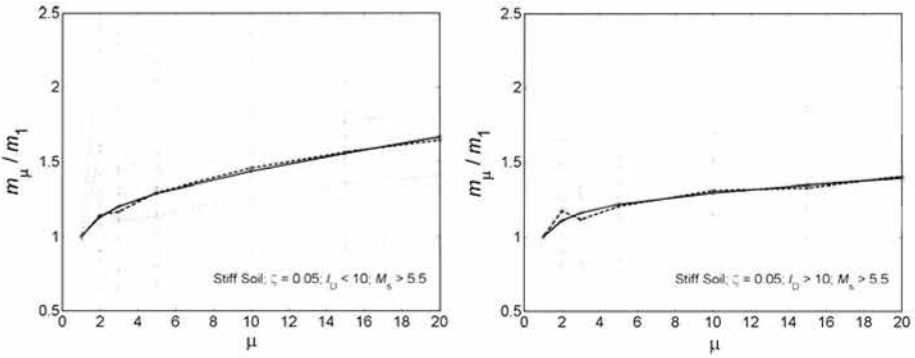

(a) Stiff soil. $M_s > 5.5$. Impulsive

(b) Stiff soil. $M_s > 5.5$. Vibratory

Fig. 6 Factor modifying the slope of the initial branch of the linear V_E spectra. $\zeta = 0.05$

Table 3 Coefficients p and s for the correction of the slopes of the initial branches of the linear V_E spectra

Soil type	Magnitude	Velocity pulses	$\zeta = 0.02$		$\zeta = 0.05$		$\zeta = 0.10$	
			p	s	p	s	p	s
Stiff soil	$M_s > 5.5$	Impulsive	0.026	0.58	0.020	0.82	0.020	0.34
		Vibratory	0.010	0.687	0.007	0.741	0.012	0.204
	$M_s \leq 5.5$	Impulsive	0.025	0.88	0.030	0.41	0.037	0.088
		Vibratory	0.014	1.052	0.017	0.58	0.014	0.60
Soft soil	$M_s > 5.5$	Impulsive	0.033	1.273	0.028	1.124	0.029	0.60
		Vibratory	0.019	0.70	0.016	0.43	0.018	0.23
	$M_s \leq 5.5$	Impulsive	0.015	1.59	0.015	1.052	0.015	0.70
		Vibratory	0.013	0.70	0.011	0.62	0.015	0.23

$r = 0.3$

displayed in Table 4 reveals that for displacement ductility larger than about 5, the value proposed by Akiyama may be unconservative.

The proposed design nonlinear V_E spectra are based on modifying the slopes of the initial branches of the linear spectra (shown in Fig. 4) with the factors listed in Table 4; the same factors are used to multiply the median and characteristic branches.

5 Comparison with other studies

In this section, the design energy input spectra proposed in this study for high seismicity regions based on Turkish ground motions are compared with those proposed by Decanini and Mollaioli (1998, 2001) and with those proposed based on registers from Colombia (Benavent-Climent et al. 2010), Iran (Amiri et al. 2008 and Greece (Tselenti et al. 2010). Furthermore, the proposed spectra are compared with those put forth under the current Japanese seismic code (BSL 2009) and by Akiyama (1985). Figure 7 shows, in solid lines, the characteristic energy input spectra proposed in this study for impulsive and vibratory earthquakes with $M_s > 5.5$ and $\mu = 1$ (see Fig. 4, Table 1 and 2) and, with thin lines, these spectra proposed by the aforementioned authors and codes. Descriptions of these comparisons are included next.

Table 4 Factors m_μ/m_1 correcting the slopes of the initial branches of the linear V_E spectra

Damping	Soil type	Magnitude	Pulses	$\mu = 2$	$\mu = 3$	$\mu = 5$	$\mu = 10$	$\mu = 15$	$\mu = 20$
$\zeta = 0.02$	Stiff soil	$M_S > 5.5$	Impulsive	1.13	1.14	1.25	1.46	1.63	1.70
			Vibratory	1.34	1.27	1.43	1.51	1.43	1.46
		$M_S \leq 5.5$	Impulsive	1.18	1.24	1.26	1.46	1.66	1.75
			Vibratory	1.17	1.22	1.27	1.39	1.50	1.54
	Soft soil	$M_S > 5.5$	Impulsive	1.24	1.25	1.35	1.60	1.77	1.91
			Vibratory	1.12	1.18	1.27	1.34	1.58	1.59
		$M_S \leq 5.5$	Impulsive	1.24	1.29	1.24	1.41	1.48	1.62
			Vibratory	1.11	1.16	1.22	1.31	1.38	1.44
$\zeta = 0.05$	Stiff soil	$M_S > 5.5$	Impulsive	1.14	1.17	1.29	1.46	1.56	1.64
			Vibratory	1.23	1.19	1.36	1.31	1.37	1.41
		$M_S \leq 5.5$	Impulsive	1.14	1.16	1.22	1.44	1.59	1.80
			Vibratory	1.11	1.13	1.25	1.37	1.45	1.57
	Soft soil	$M_S > 5.5$	Impulsive	1.21	1.23	1.30	1.57	1.70	1.78
			Vibratory	1.15	1.15	1.20	1.26	1.41	1.56
		$M_S \leq 5.5$	Impulsive	1.13	1.23	1.31	1.41	1.46	1.59
			Vibratory	1.11	1.16	1.22	1.30	1.35	1.39
$\zeta = 0.10$	Stiff soil	$M_S > 5.5$	Impulsive	1.15	1.10	1.17	1.30	1.50	1.55
			Vibratory	1.19	1.14	1.24	1.25	1.32	1.37
		$M_S \leq 5.5$	Impulsive	1.08	1.11	1.16	1.37	1.57	1.77
			Vibratory	1.18	1.09	1.22	1.34	1.43	1.51
	Soft soil	$M_S > 5.5$	Impulsive	1.17	1.16	1.27	1.45	1.67	1.80
			Vibratory	1.04	1.14	1.14	1.23	1.41	1.47
		$M_S \leq 5.5$	Impulsive	1.17	1.21	1.18	1.36	1.47	1.56
			Vibratory	1.04	1.07	1.12	1.20	1.28	1.35

- **Spectra from Colombian registers**. Figure 7a shows the design energy input spectra proposed in (Benavent-Climent et al. 2010) based on 144 Colombian registers associated with design PGA equal to 0.4 g. These authors considered three soil types: rock (shear wave velocity $v_s > 750$ m/s), stiff soil ($375 \leq v_s \leq 750$ m/s) and intermediate soil ($175 \leq v_s \leq 375$ m/s). As seen in the figure, the levels of input energy proposed in this study are approximately bounded by the levels adopted from Colombian records for soils type I and II.
- **Spectra from the Japanese code**. Figure 7b shows with thin lines the design energy input spectra V_E prescribed by the current Japanese seismic code BSL (2009) to be used in conjunction with earthquake-resistant structural calculation based on energy balance. The BSL code classifies the surface geology in three types: (i) soil 1 is rock, stiff sand gravel, and pre-Tertiary deposits; (ii) soil 3 includes alluvial layers mainly consisting of humus and mud whose depth is over 30 m, or filled land more than 3 meters deep and worked within the past 30 years; (iii) soil 2 comprises layers other than types 1 and 3. The BSL code directly gives the V_D spectra. For comparison with the spectra proposed in this study, V_E was estimated from V_D using the proposed Eq. (17) particularized for a vibratory earthquake with $M_S > 5.5$, and assuming $\zeta = 0.05$ and $\eta = 15$ (Table 5). The levels of V_E prescribed by BSL and those proposed in this study are similar in the medium period range (i.e. in the region where V_E is constant). However, in the short and large period ranges the levels prescribed by BSL are smaller and larger, respectively, than those proposed in this study. The levels put forth here for impulsive earthquakes are clearly larger than those proposed by the BLS code.

- **Spectra from** (Akiyama 1999). Figure 7c shows in thin lines the design energy input spectra proposed by Akiyama (1999) for Japan, considering four types of surface geology. Soil type I corresponds to hard rock or very hard conglomerates (shear wave velocity $v_s > 750$ m/s); type II corresponds to hard conglomerates, compact sand and gravel with $375 \leq v_s \leq 750$ m/s; type III corresponds to intermediate soils such as semi-compact sands and gravels with $175 \leq v_s \leq 375$ m/s; and type IV corresponds to soft soils with $v_s \leq 175$ m/s. In the medium period range (i.e. the range where V_E is constant) the spectra proposed in this study are close to those proposed by Akiyama.
- **Spectra from Iranian registers**. Figure 7d shows the design energy input spectra proposed by Amiri et al. (2008) based on 110 Iranian earthquakes. These authors consider four types of soil (I, II, III and IV), corresponding to rock, stiff, medium and soft soil, respectively. It can be seen that the spectra proposed in this study for vibratory registers are approximately 30 % larger in stiff soil and about 45 % larger in soft soil, than those suggested by Amiri et al. For impulsive earthquakes the levels proposed in this study are roughly two times greater than those proposed by Amiri et al. It is worth noting that both regions (Iran and Turkey) have similar seismicity and the maximum design PGA in the Turkish seismic code (0.4 g) is similar to that of the Iranian code (0.35 g). The biggest discrepancy with the spectra proposed by Amiri et al. corresponds to the impulsive registers. Such disagreement might be due to the scarcity of near-fault registers in their study. Further discrepancies may be attributed to statistical criteria: this work establishes the design spectra corresponding to the top 95 % percentile, while Amiri et al. take the average plus one standard deviation; if normality is assumed, this level would correspond to the 84 % percentile.
- **Spectra from Greek registers**. Figure 7e shows the V_E spectra proposed by Tselenti et al. (2010) for six cities in Greece by means of a methodology unlike ours. These authors adopt the probabilistic approach originally developed by Cornell (1968) and extended later by Esteva (1970). Each city has a different design PGA (0.16 g for Athens and Thessaloniki; 0.24 g for Patras, Korinthos and Chania; and 0.36 g for Argostolion), which varies in approximately the same range as the Turkish seismic code (i.e. from 0.15 g to 0.4 g). As observed in the figure, the spectra proposed by Tselenti et al. (2010) for these cities would match the spectra developed in this study for vibratory records and for stiff and soft soil quite well.
- Decanini and Mollaioli (1998, 2001). Decanini and Mollaioli (1998) proposed general shapes for design energy input spectra, normalized by the Seismic Hazard Factor AE_I. These authors proposed different values for AE_I depending on the surface geology conditions, the interval of surface-wave magnitude M_S and the epicentral distance R_{epi}. For 12 km $< R_{epi} <$ 30 km and $6.5 \leq M_S \leq 7.1$, Decanini and Mollaioli proposed AE_I = 16,000 cm^2/s for soil type S1 and AE_I = 50,000 cm^2/s for soil type S2; this is identified as the vibratory register. For $R_{epi} < 5$ km and $6.5 \leq M_S \leq 7.1$, Decanini and Mollaioli proposed AE_I = 65,000 cm^2/s for soil type S1 and AE_I = 110,000 cm^2/s for soil type S2; this is identified as the impulsive register. The design energy input spectra obtained by substituting these values of AE_I in the normalized spectra considered by Decanini and Mollaioli (1998) for $\mu = 1$ are drawn in Fig. 7f. In the medium period range (i.e. constant input energy range) the levels of V_E proposed in this study are seen to be similar to those of Decanini and Mollaioli; although the descending branches begin earlier in their case, the rate of stabilization of the slope is higher.

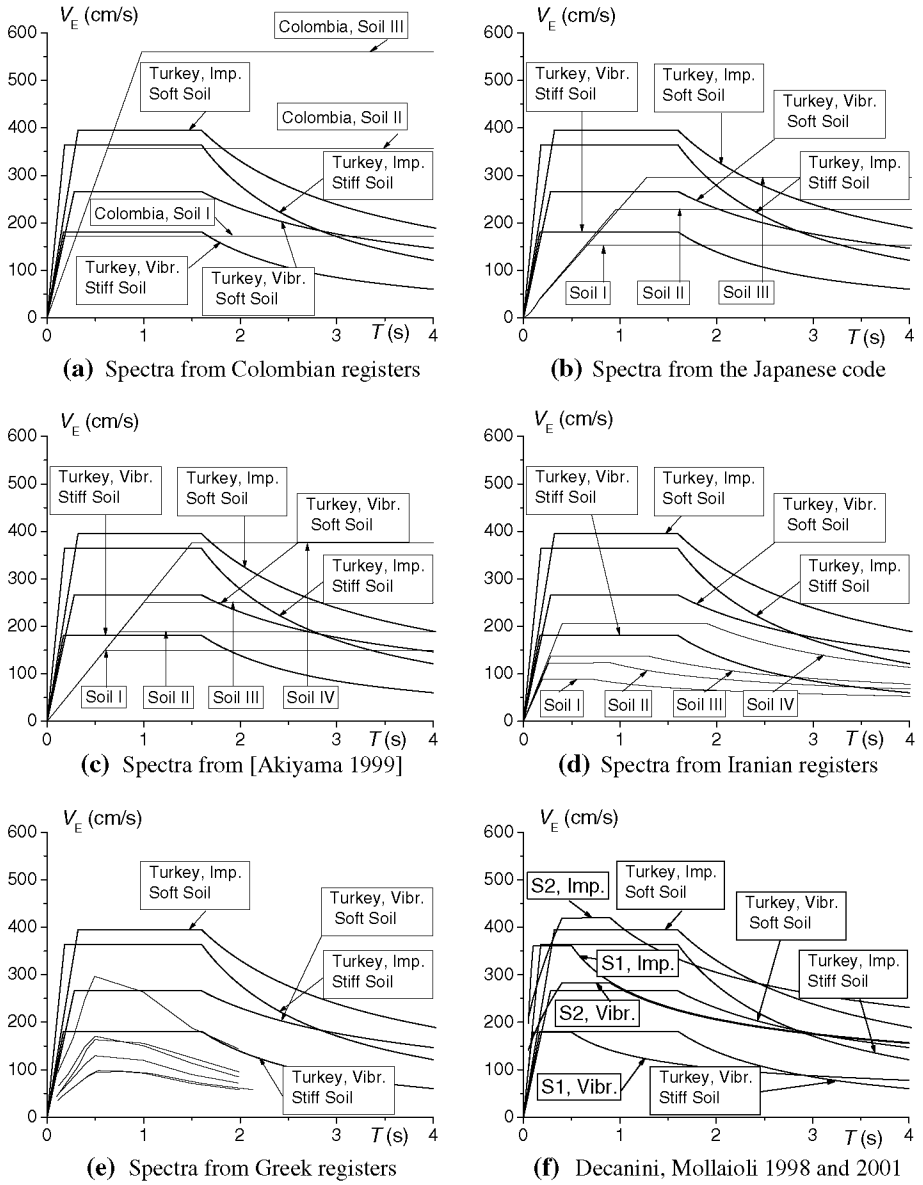

Fig. 7 Comparison among the proposed spectra and those from other studies

6 Design hysteretic energy to input energy ratio V_D / V_E

6.1 Introductory remarks

The evaluation of the input energy E_I is an acceptable starting point to develop and apply the seismic energy-based design methods. However, only hysteretic energy E_H (alike E_D, according to Eq. (5)) is directly related to seismic structural damage, and must be evaluated

(Manfredi 2001). Since V_D and E_H are directly related by Eq. (6), estimation of the ratio V_D/V_E, in view of the non-linear analyses presented in Subsect. 4.3, is described below.

6.2 Previous studies

As discussed in Sect. 2, V_D/V_E depends mainly on the structural damping and on the demanded ductility; the latter can be formulated in terms of the displacement ductility μ, or in terms of the cumulative ductility η:

$$\mu = \frac{y_{max}}{y_y} \quad \eta = \frac{E_H}{Q_y y_y} \tag{13}$$

In Eq. (13), y_{max} is the maximum displacement and Q_y and y_y are the restoring force and the displacement at yielding, respectively. Several empirical equations have been proposed in the literature to estimate V_D/V_E. Based on analyses of SDOF systems with elastic-perfectly-plastic restoring force characteristics, Akiyama (1985) and Kuwamura and Galambos (1989) respectively presented the following equations:

$$\frac{V_D}{V_E} = \frac{1}{1 + 3\zeta + 1.2\sqrt{\zeta}} \quad \frac{V_D}{V_E} = \frac{\frac{\eta}{\eta+0.15}}{1 + \frac{20(3\zeta+1.2\sqrt{\zeta})}{\eta+10}} \tag{14}$$

In turn, Benavent et al. (2002,2010) suggested, respectively, the following modifications of the (left) Akiyama Eq. (14) to account for the level of plastification:

$$\frac{V_D}{V_E} = \frac{1.15\eta}{(0.75+\eta)(1 + 3\zeta + 1.2\sqrt{\zeta})} \quad \frac{V_D}{V_E} = \frac{1}{\sqrt{1+4\pi\zeta n}} \frac{\eta^c}{(8.75\zeta + k^c + \eta^c)} \tag{15}$$

In the last Eq. (15), n, k and c are dimensionless coefficients whose values are $n = 0.9$, $k = 0.33$ and $c = 0.57$ for rock, and $n = 0.15$, $k = 0.02$ and $c = 0.37$ for soil.

From parametric studies with non-linear elastic-perfectly-plastic SDOF systems, Fajfar and Vidic (1994) proposed an expression valid for systems with $\zeta = 0.05$:

$$\frac{V_D}{V_E} = \sqrt{\frac{0.9\,(\mu-1)^{0.95}}{\mu}} \tag{16}$$

Lawson and Krawinkler (1995) confirmed that V_D/V_E constitutes a highly stable parameter, and proposed adopting $V_D/V_E = 0.63$ for $\mu = 2$ and $V_D/V_E = 0.77$ for $4 \leq \mu \leq 8$, except for the shortest periods. Decanini and Mollaioli (2001) investigated the ratio $E_H/E_{I,abs}$ in relation with the period T, the type of soil, and the ductility μ for elastic-perfectly-plastic SDOF systems with $\zeta = 5\,\%$; Although Akiyama used the relative input energy and Decanini and Mollaioli the absolute input energy, the design values of the ratio of hysteretic energy to total input energy proposed by both approaches are comparable. Decanini and Mollaioli moreover investigated the effects of the hysteretic model, the vibration period, and the soil type.

6.3 Influence of damping and ductility

In this study, the registers were classified into eight groups, depending on the soil type, the earthquake magnitude and the relevance of the velocity pulses (Sect. 3). Mainly for this reason, we develop a new empirical approximation of V_D/V_E whose parameters take such diversity into account. This expression is intended to be used together with the spectra proposed in Sect. 4. The agreement between the obtained points and previously suggested fits

is reasonable (Yazgan 2012), particularly a recent study by Benavent-Climent et al. (2010). However, the fit can be further improved and, moreover, no previous study looked into the influence of soil type, earthquake magnitude, velocity pulses and period to such an extent. For this reason, another fitting criterion is proposed here. To derive such criteria, Fig. 8 shows the obtained points for damping 5%; the reference (Yazgan 2012) contains similar results for damping 2 and 10%. These points are plotted together with the best fit curve using a two-term exponential expression:

$$\frac{V_D}{V_E} = ae^{b\eta} + ce^{d\eta} \tag{17}$$

This expression is chosen given its suitability to the clouds of points to be fitted. In the second term of Eq. (17), coefficients c ("amplitude") and d ("exponent") are intended to be negative and provide the trend of the fitting curves to be horizontal for $\eta > 100$; in the first term amplitude a is positive and exponent b can be either negative or positive. The absolute values of the exponent b are significantly smaller than those of d, while this trend is inverted for the amplitudes. Roughly, the first term governs the behavior for small values of η whereas the second term controls the values for higher values of η.

Table 5 shows the values of the coefficients a, b, c and d that provide the best fit in the sense of the least value of the sum of the squares of the differences between the ordinates of the obtained points and those of the fitting curves.

Table 5 shows the following general trends: (i) V_D/V_E increases with the increase of η, but this dependency tends to disappear as the parameter grows; (ii) V_D/V_E decreases with the increase of ζ; (iii) for a given value of η, the dispersion of V_D/V_E increases with ζ and, for a given value of ζ, the dispersion of V_D/V_E decreases with η; (iv) the overall behavior of V_D/V_E for impulsive and vibratory registers is quite similar, although for smaller η the values of V_D/V_E are slightly higher for impulsive registers than for vibratory ones; (v) the results for $M_s > 5.5$ and for $M_s \leq 5.5$ are roughly equivalent; and (vi) V_D/V_E is similar in stiff soil and in soft soil. These last three conclusions show that the ratio V_D/V_E is analogous in the eight groups analyzed (Sect. 3); therefore, the proposal of approximate expressions for estimating V_D/V_E can be made irrespectively of soil type, impulsivity of the register and magnitude of the earthquake. Figure 9 displays the clouds of points corresponding to all the considered registers (Table 9) for damping factors $\zeta = 0.02$, 0.05 and 0.10 together with the best fit curves according to the two-term exponential expression (17). Figure 9a–c show the cases for $\zeta = 0.02$, 0.05 and 0.10, respectively, while Fig. 9d shows jointly the three exponential fitting curves alone (e.g. without the fitted points). In addition, Table 6 displays the values of the coefficients a, b, c and d that provide the best fit for $\zeta = 0.02$, 0.05 and 0.10.

6.4 Influence of period

To assess the variation of ratio V_D/V_E with period T, Fig. 10 shows the spectra of V_D/V_E for different values of the damping factor ($\zeta = 0.02, 0.05$ and 0.10) and of displacement ductility ($\mu = 2$, 3, 5, 10, 15 and 20). Since the previous study about the influence of ζ and η on the V_D/V_E ratio (Subsect. 6.3) points to little influence of the soil type, the impulsive/vibratory character and the earthquake magnitude, the V_D/V_E spectra are presented herein regardless of these aspects; in other words, each set of plots in Fig. 10 corresponds to all the registers in Table 9. Figure 10a through Fig. 10r illustrate the individual spectra, the median and a linear fit of the median spectrum. Remarkably, a bilinear approximation (where the initial branch starts from $V_D/V_E = 1$ for $T = 0$) would provide a better match; however, since that branch

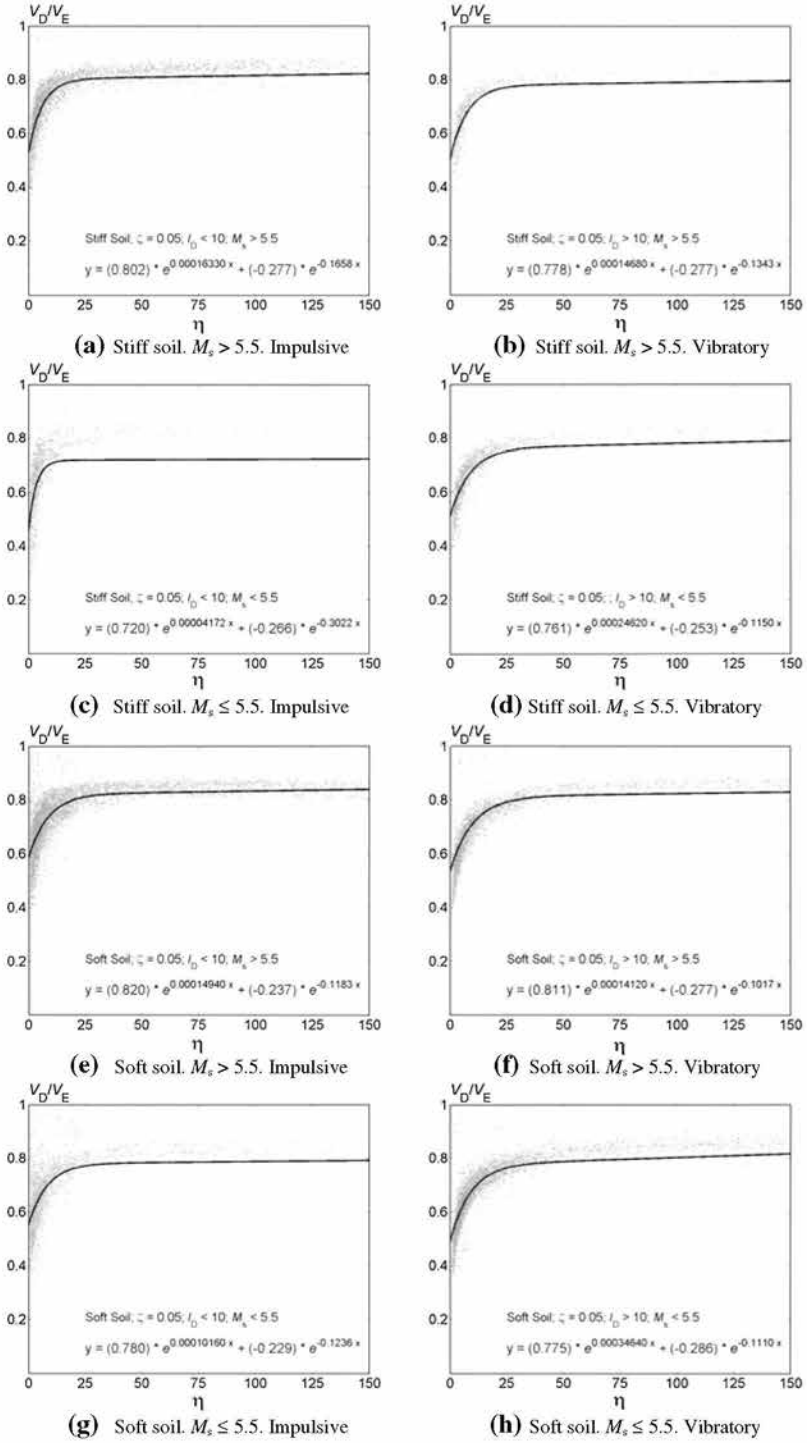

Fig. 8 Proposed empirical approximations of the ratio V_D/V_E for damping $\zeta = 0.05$

Table 5 Coefficients of the best exponential fit curve of the V_D/V_E ratio for each group

Damping	Soil type	Magnitude	Pulses	a	b	c	d
$\zeta = 0.02$	Stiff soil	$M_s > 5.5$	Imp.	0.893	0.0001885	−0.243	−0.180
			Vibr.	0.877	0.0001867	−0.236	−0.156
		$M_s \leq 5.5$	Imp.	0.879	−0.0000235	−0.291	−0.262
			Vibr.	0.866	0.0002698	−0.219	−0.142
	Soft soil	$M_s > 5.5$	Imp.	0.904	−0.000000757	−0.219	−0.146
			Vibr.	0.898	0.0001648	−0.229	−0.118
		$M_s \leq 5.5$	Imp.	0.880	0.0000201	−0.206	−0.140
			Vibr.	0.878	0.0002496	−0.247	−0.131
$\zeta = 0.05$	Stiff soil	$M_s > 5.5$	Imp.	0.802	0.0001633	−0.277	−0.166
			Vibr.	0.777	0.0001467	−0.277	−0.134
		$M_s \leq 5.5$	Imp.	0.720	0.0000417	−0.266	−0.302
			Vibr.	0.761	0.0002462	−0.252	−0.115
	Soft soil	$M_s > 5.5$	Imp.	0.820	−0.0001494	−0.273	−0.118
			Vibr.	0.811	0.0001412	−0.277	−0.102
		$M_s \leq 5.5$	Imp.	0.780	−0.0001016	−0.229	−0.124
			Vibr.	0.775	0.0003464	−0.286	−0.111
$\zeta = 0.10$	Stiff soil	$M_s > 5.5$	Imp.	0.704	0.00004824	−0.276	−0.152
			Vibr.	0.673	0.00004073	−0.266	−0.109
		$M_s \leq 5.5$	Imp.	0.607	−0.0001398	−0.231	−0.272
			Vibr.	0.665	0.0000176	−0.252	−0.086
	Soft soil	$M_s > 5.5$	Imp.	0.732	−0.0000412	−0.239	−0.098
			Vibr.	0.702	0.00001194	−0.284	−0.089
		$M_s \leq 5.5$	Imp.	0.710	−0.0003608	−0.259	−0.096
			Vibr.	0.665	0.0004298	−0.281	−0.099

corresponds only to extremely short periods (e.g. shorter than 0.06 s), it is neglected in this study. Table 7 displays the parameters of the chosen linear fit: the slope, the spectral ordinate corresponding to $T = 4$ s, and the average spectral ordinate, e.g. the one that corresponds to $T = 2$ s.

Taken together, the plots from Fig. 10 and data from Table 7 reflect the overall trends of damping and of ductility influence outlined earlier (the V_D/V_E ratio decreases with increasing damping and increases with increasing ductility). The results in Table 7 moreover show that the slope increases with damping, and the dependency of the slope on ductility also increases with damping; roughly, it grows as ductility does. The spectral ordinates corresponding to periods 2 and 4 s are seen to increase with ductility while decreasing with damping.

As shown next, the fits of Fig. 10 and those of Decanini and Mollaioli (2001) generally agrees, except in the short period range. This difference stems from the conception of absolute energy. Decanini and Mollaioli propose a trilinear E_H/E_I spectrum characterized, among other parameters, by e, f and T_3, with e as the maximum spectral ordinate, f the ordinate at $T = 4$ s, and T_3 the period that determines the onset of the horizontal branch. Parameters e and f (see Fig. 16 and Table 11 in (Decanini and Mollaioli 2001)) can be compared, for $\zeta = 0.05$, to the squares of the spectral ordinates corresponding to T_3 (ranging between 0.225 and 0.55 s) and to 4 s, respectively (Fig. 10 and Table 7). Meanwhile, Table 8 offers a comparison of the values of the square roots of e and f and those of the aforementioned spectral ordinates. The second and fourth columns of Table 8 ($\overline{e}$ and spectral ordinate for period T_3) show satisfactory agreement, yet the third and fifth columns ($\overline{f}$ and spectral ordinate for 4 s) show poorer agreement, the proposed fit being more conservative.

The common assumption that V_D/V_E is roughly independent of period is no longer sustainable in view of Fig .10 and Table 7. In contrast, the approximation given by Eq. (17)

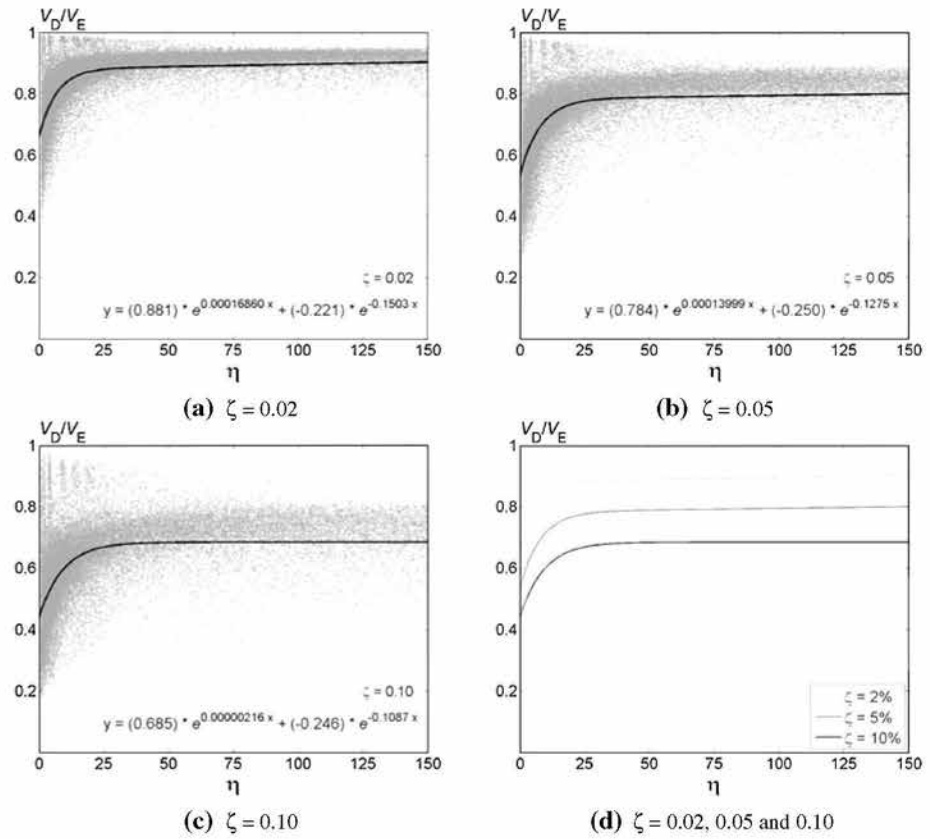

(a) $\zeta = 0.02$ **(b)** $\zeta = 0.05$

(c) $\zeta = 0.10$ **(d)** $\zeta = 0.02$, 0.05 and 0.10

Fig. 9 Proposed empirical approximations of the ratio V_D/V_E regardless of the group

Table 6 Coefficients of the best exponential fit curve of the V_D/V_E ratio for all the groups

Damping	a	b	c	d
$\zeta = 0.02$	0.881	0.00016860	−0.221	−0.1503
$\zeta = 0.05$	0.784	−0.00013999	−0.250	−0.1275
$\zeta = 0.10$	0.685	0.00000216	−0.246	−0.1087

(with the values of the coefficients a, b, c and d listed in Table 6) corresponds to the average ordinate of the fits shown in Fig. 10 and listed in Table 7.

6.5 Proposed criteria for estimating V_D/V_E

The previous two subsections describe criteria for estimating the V_D/V_E ratio in terms of period T, ductility μ or η, and damping ζ. Subsection 6.4 provides criteria that depend on T, μ and ζ; while the study expounded in Subsect. 6.3 illustrates the influence of η and ζ but must be complemented with Subsect. 6.4 to incorporate the effect of T. Accordingly, the first proposed criterion consists of the linear decreasing spectra drawn in Fig. 10 (the values of the parameters of the linear fit are listed in Table 7 in terms of μ and ζ). The second proposed

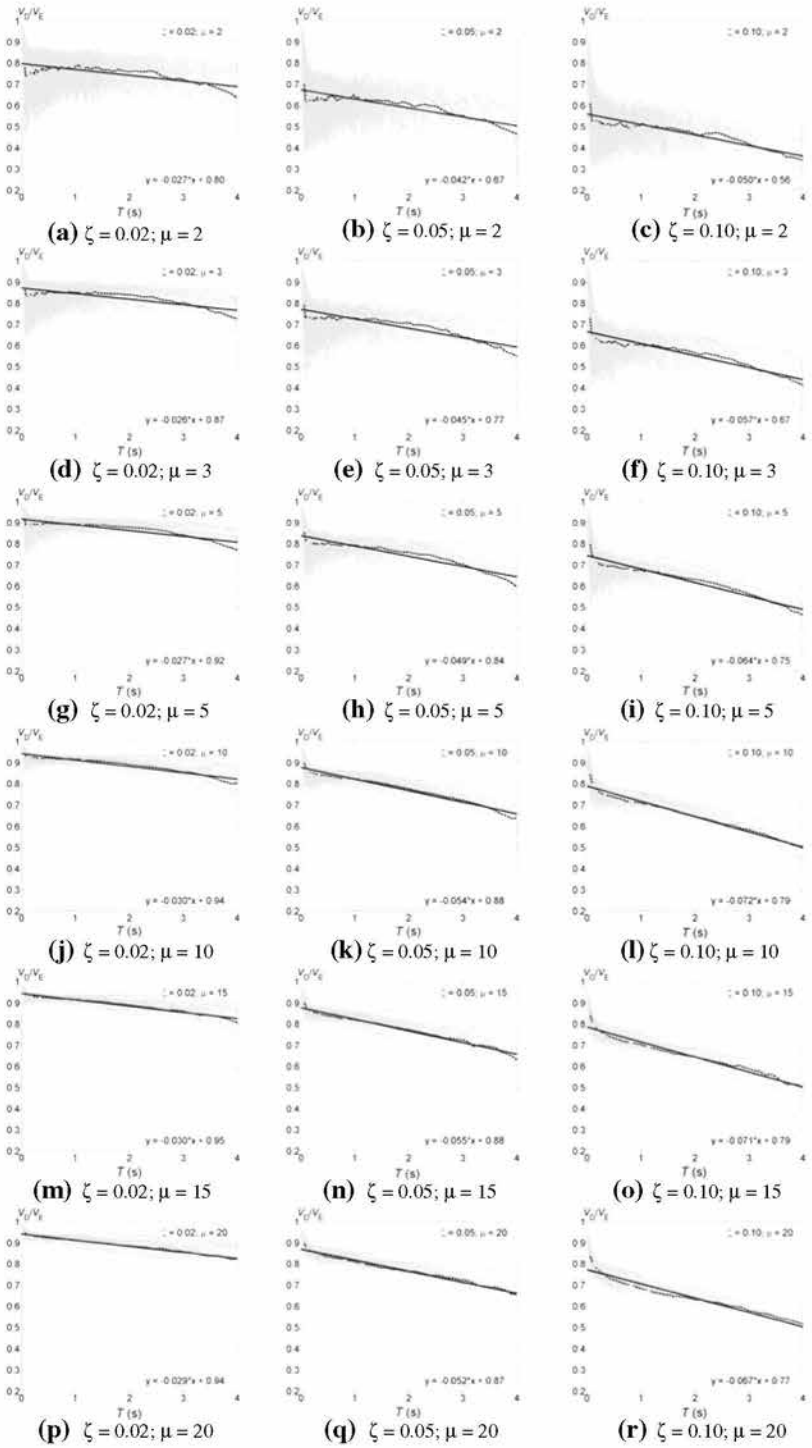

Fig. 10 Spectra of the ratio V_D / V_E

Table 7 Parameters for the linear fit of the V_D/V_E spectra

ζ	μ	Slope (s^{-1})	Spectral ordinate ($T = 4$ s)	Average spectral ordinate ($T = 2$ s)
0.02	2	−0.027	0.692	0.746
	3	−0.026	0.766	0.818
	5	−0.027	0.812	0.866
	10	−0.030	0.820	0.880
	15	−0.030	0.830	0.890
	20	0.029	0.824	0.882
0.05	2	−0.042	0.502	0.586
	3	−0.045	0.590	0.680
	5	0.049	0.644	0.742
	10	−0.054	0.664	0.772
	15	−0.055	0.660	0.770
	20	−0.052	0.662	0.766
0.10	2	−0.050	0.360	0.460
	3	−0.057	0.442	0.556
	5	−0.064	0.494	0.622
	10	−0.072	0.502	0.646
	15	−0.071	0.506	0.648
	20	−0.067	0.502	0.636

Table 8 Comparison among the parameters for the proposed linear fit of the V_D/V_E spectra (for $\zeta = 0.05$) and the one by Decanini and Mollaioli (2001)

μ	$\overline{e}$ (stiff soil / soft soil)	$\overline{f}$ (stiff soil / soft soil)	Spectral ordinate (T_3) (stiff soil / soft soil)	Spectral ordinate ($T = 4$ s)
2	0.693 / 0.707	0.632 / 0.686	0.657 / 0.645	0.502
3	0.742 / 0.758	0.671 / 0.731	0.758 / 0.745	0.590
5	0.800 / 0.822	0.714 / 0.781	0.829 / 0.817	0.644

criterion consists of the two-term exponential curves plotted in Fig. 9d and described in Table 6, multiplied by the ratio between the ordinate corresponding to the considered period and the average spectral ordinate (Fig. 10 and Table 7). Since there is no direct relation between μ and η, the two proposed criteria are not equivalent.

The V_D spectra can be obtained by multiplying the V_D/V_E spectra put forth in this subsection by the three-branched V_E spectra (linear spectra depicted in Fig. 5 and nonlinear modification of the initial branches described in Table 4).

The suitability of each criterion described here depends mainly on whether the energy dissipation capacity is characterized in terms of displacement ductility μ or cumulated ductility η. The second criterion would be preferable in the particular case of designing structures with hysteretic dampers.

7 Conclusions

This work proposes design input energy spectra formulated in terms of velocity (V_E), especially appropriate for regions with design peak ground acceleration equal or higher than 0.3 g. They were obtained from a number of Turkish records from zones with PGAs of this magnitude.

The proposed spectra are derived through linear and nonlinear dynamic analyses for selected Turkish registers. In the long and mid period ranges, due to the relative insensitivity of the spectra to the structural parameters other than the fundamental period, the analyses are linear. Contrariwise, in the short period range, the spectra are more sensitive to the structural parameters and call for nonlinear analyses. The selected Turkish records, classified in eight groups with respect to the soil type (stiff and soft soil), the magnitude of the earthquake ($M_S \leq 5.5$ and $M_S > 5.5$) and the relevance of the near-source effects (impulsive and vibratory registers), give rise to median and characteristic spectra for each group, with levels intended to correspond to the 50 and 95 % percentiles, respectively. The proposed spectra have an initial linear growing branch in the short period range, a horizontal branch in the mid period range and a descending branch in the long period range. For nonlinear design, in each of the eight groups, empirical criteria are proposed to modify the slope of the initial branch according to the displacement ductility; the same criteria are considered for the median and characteristic spectra.

Empirical criteria for estimating the ratio between hysteretic energy in terms of velocity (V_D) and input energy (V_E) are presented. Although these criteria depend on period, damping and ductility; displacement and cumulated ductility are considered as well. It should be stressed that the influence of period is considered relevant, yet the influence of the parameters that characterize each group (soil type, earthquake magnitude and impulsivity) is negligible.

When compared with those obtained from other studies, the proposed design spectra are in some cases greater while in other cases they are smaller. Overall, no noteworthy differences are observed.

Acknowledgments This work received financial support from the Spanish Government under projects CGL2008-00869/BTE, CGL2011-23621, BIA2008-00050 and BIA2011-26816 and from the European Union (FEDER). The stay of Dr. Yazgan in Barcelona was funded by the Spanish Government (Ministry of Foreign Affairs) "Becas MAE-AECID" Grant No. 447958.

References

Adang S (2007) Earthquake-resistant structural design through energy demand and capacity. Eng Struct Dyn 36:2099–2117. doi:10.1002/eqe.718

Akiyama H (1985) Earthquake-resistant limit-state design for buildings. University of Tokyo Press, Tokyo

Akiyama H (1999) Earthquake-resistant design method for buildings based on energy balance. Gihodo Shuppan: 25–26

Akkar S, Çagnan Z, Yenier E, Erdogan Ö, Sandıkkaya MA, Gülkan P (2010) The recently compiled Turkish strong motion database: preliminary investigation for seismological parameters. J Seismol 14(3):457–479

Amiri GG, Darzi GA, Amiri JV (2008) Design elastic input energy spectra based on Iranian earthquakes. Can J Civ Eng 35:635–646

Arias A (1970) A measure of earthquake intensity. Seismic design for nuclear power plants. In: Hansen R (ed) MIT Press, Cambridge, pp 438–483

Baker JW (2007) Quantitative classification of near-fault ground motions using wavelet analysis. Bull Seismol Soc Am 97(5):1486–1501

Benavent-Climent A (2007) An energy-based damage model for seismic response of steel structures. Earthq Eng Struct Dyn 36:1049–1064

Benavent-Climent A, Pujades LG, López-Almansa F (2002) Design energy input spectra for moderate-seismicity regions. Earthq Eng Struct Dyn 31:1151–1172

Benavent-Climent A, López-Almansa F, Bravo DA (2010) Design energy input spectra for moderate-to-high seismicity regions based on Colombian earthquakes. Soil Dyn Earthq Eng 30(11):1129–1148

Berg GV, Thomaides SS (1960) Energy consumption by structures in strong-motion earthquakes. Proc Second World Conf Earthq Eng 2:681–697

Bertero RD, Bertero VV, Teran-Gilmore A (1996) Performance-based earthquake-resistant design based on comprehensive design philosophy and energy concepts. In: Proceedings of the eleventh world conference on earthquake engineering, Disc 2, Paper No. 611

Bruneau M, Wang N (1996) Normalized energy-based methods to predict the seismic ductile response of SDOF structures. Eng Struct 18:13–28

BSL. The building standard law of Japan. (2009). The building center of Japan, Tokyo. (English version on CD available at http://118.82.115.195/en/services/publication.html)

Chou CC, Uang CM (2000) Establishing absorbed energy spectra -an attenuation approach-. Earthq Eng Struct Dyn 29:1441–1455

Chou CC, Uang CM (2003) A procedure for evaluating seismic energy demand of framed structures. Earthq Eng Struct Dyn 32:229–244

Cornell CA (1968) Engineering seismic risk analysis. Bull Seismol Soc Am 58:1583–1606

Cosenza E, Manfredi G, Polese M (2009) A simplified method to include cumulative damage in the seismic response of SDOF systems. J Eng Mech ASCE 135(10):1081–1088

Decanini LD, Mollaioli F (1998) Formulation of elastic earthquake input energy spectra. Earthq Eng Struct Dyn 27:1503–1522

Decanini LD, Mollaioli F (2001) An energy-based methodology for the seismic assessment of seismic demand. Soil Dyn Earthq Eng 21:113–137

EN 1998. (2004) Eurocode 8. Design of structures for earthquake resistance, European Committee for Standarization

Erdogan Ö (2008) Main seismological features of recently compiled Turkish strong motion database. MSc Thesis. Middle East Technical University, Ankara, Turkey

Esteva L (1970) Seismic risk and seismic design decision, seismic design for nuclear power plants. MIT Press, Cambridge, pp 142–182

Fajfar P, Vidic T (1994) Consistent inelastic design spectra: hysteretic and input energy. Earthq Eng Struct Dyn 23:523–537

Hall WL, Nau JM, Zahrah TF (1984) Scaling of response spectra and energy dissipation in SDOF systems. In: Proceedings of the eighth world conference on earthquake engineering, vol 4, pp 7–14

Housner GW (1956) Limit design of structures to resist earthquakes. Proc First World Conf Earthq Eng 5:1–12

Housner GW, Jennings PC (1977) The capacity of extreme earthquake motions to damage structures, structural and geotechnical mechanics, a volume honoring Nathan M. Newmark, pp 102–116

Iervolino I, Manfredi G, Cosenza E (2006) Ground motion duration effects on nonlinear seismic response. Earthq Eng Struct Dyn 35:21–38

Jiao Y, Yamada S, Kishiki S, Shimada Y (2011) Evaluation of plastic energy dissipation capacity of steel beams suffering ductile fracture under various loading histories. Earthq Eng Struct Dyn 40:1553–1570. doi:10.1002/eqe.1103

Kato B, Akiyama H (1975) Energy input and damages in structures subjected to severe earthquakes. J Struct Constr Eng Trans AIJ 235:9–18 (in Japanese)

Kempton JJ, Stewart JP (2006) Prediction equations for significant duration of earthquake ground motions considering site and near-source effects. Earthq Spectra 22(4):985–1013

Kuwamura H, Galambos TV (1989) Earthquake load for structural reliability. J Struct Eng ASCE 115(6):1446–1462

Kuwamura H, Kirino Y, Akiyama H (1994) Prediction of earthquake energy input from smoothed fourier amplitude spectrum. Earthq Eng Struct Dyn 23:1125–1137

Lawson RS, Krawinkler H (1995) Cumulative damage potential of seismic ground motion. In: Proceedings of the 10th European conference on, earthquake engineering 1079–86

Leelataviwat S, Saewon W, Goel SC (2009) Application of energy balance concept in seismic evaluation of structures. J Struct Eng 135(2):113–121

Manfredi G (1995) Stime energetiche e potenziale di danno sismico, VII Convegno Nazionale: L'Ingenieria sismica in Italia. Siena. 1:43–52

Manfredi G (2001) Evaluation of seismic energy demand. Earthq Eng Struct Dyn 30:485–499

Priestley MJN, Calvi GM, Kowalsky MJ (2007) Displacement-based seismic design of structures, IUSS Press

Teran-Gilmore A (1996) Performance-based earthquake-resistant design of framed buildings using energy concepts, PhD Thesis, Department of Civil Engineering, University of California at Berkeley

Triffunac MD, Brady AG (1975) A study on the duration of strong earthquake ground motion. Bull Seism Soc Am 65(3):581–626

TSC 2007 (2007) Ministry of public works and settlement of Turkey, Turkish Seismic Code. Specification for Buildings to be constructed in Seismic Zones

Tselentis GA, Danciu L, Sokos E (2010) Probabilistic seismic hazard assessment in Greece. Part II: acceleration response spectra and elastic input energy spectra. Nat Hazards Earth Sci Syst 10:1–15

Uang CM, Bertero VV (1988) Use of energy as a design criterion in earthquake-resistant design. Report No. UBC-EERC-88-18. Berkeley: Earthquake Engineering Research Center, University of California
Uang CM, Bertero VV (1990) Evaluation of seismic energy in structures. Earthq Eng Struct Dyn 19(1):77–90
UBC (1997) Uniform building code. International council of building officials
Yazgan AU (2012) Proposal of energy spectra for earthquake resistant design based on Turkish registers. Technical University of Catalonia, Doctoral Dissertation
Yei L, Otani S (1999) Maximum seismic displacement of inelastic systems based on energy concept. Earthq Eng Struct Dyn 28:1483–1499
Zahrah TF, Hall WJ (1984) Earthquake energy absorption in SDOF systems. J Struct Eng 110:1757–1772